

A NEW INTERPRETATION OF FATIGUE CRACK GROWTH

A. K. Vasudevan¹ and K. Sadananda²

The fatigue crack growth behavior in materials has been described in terms of two load parameters that are independent of crack closure, but depend on the microstructure and environment. The overall fatigue behavior is classified into five classes based on the basic ΔK -R curves requiring the understanding of the synergistic effects of the mechanical driving forces (in terms of the two loading parameters) and the chemical driving forces due to the environment.

INTRODUCTION

It is well known that there is a threshold stress intensity ΔK_{th} , below which a fatigue crack cannot grow. The value of this threshold depends on many factors that include material properties, microstructure, load ratio, load history and environment. During the past twenty years, the above variables affecting the threshold have been explained by using the crack closure concept, widely held by many researchers, yet poorly understood. We have recently reexamined the threshold behavior in many materials and found that the closure contributions are not significant and that the behavior can be explained by considering two stress intensity parameters (ΔK_{th} & K_{max}) that are to be met simultaneously for the crack to advance

¹ Office of Naval research, Code 4421, Arlington, VA 22217

² Naval Research Lab., Code 6323, Washington D.C. 20375

(1-6). Based on these concepts, the entire crack growth behaviors can be classified into five groups that depends on the fatigue deformation characteristics. The article, briefly discusses these topics giving appropriate examples in each case as pertinent.

CRACK CLOSURE

In the absence of crack closure, the crack tip driving force is related to the applied stress intensity ΔK_{app} ($= K_{max} - K_{min}$). When closure is present, the driving force is decreased to an effective amplitude $\Delta K_{eff} = K_{max} - K_{cl}$, where K_{cl} is the stress intensity where crack closure occurs. Major support for the closure concept comes from the observation that the fatigue crack growth rates (da/dN) can be compressed to a narrow band when the data from different load ratios ($R=K_{min}/K_{max}$) were plotted in terms of ΔK_{eff} rather than ΔK_{app} . This implies that the fatigue threshold values and growth rates depend on the effective driving force ΔK_{eff} than the applied driving force ΔK_{app} . This would be a problem for a structural engineer, since the closure loads are difficult/impossible to obtain for a service component, as they are system/application specific.

To resolve such a problem, we have critically reexamined the crack closure concepts and the sources that are believed to contribute to the crack closure, using the basic concepts from dislocation theory. Crack-tip plasticity, oxidation or corrosion products in the crack wake, and asperities from crack path are all believed to be the major sources of crack closure (7). Our analyses show the following : (a) plasticity does not contribute to crack closure since the crack opening displacements are always greater than the crack closing displacements; (b) complete closure can occur only when the crack volume is completely filled with an oxide or a corrosion product (not experimentally observed); (c) asperities occur randomly and as a result asperity-induced closure cannot explain the seemingly deterministic behavior of the systematic dependence of ΔK_{th} on R, and finally, (d) partial closure can occur locally at the asperities, but their effects are nominal on the crack-tip stress fields. Thus, in most cases,

crack closure is either non-existent or insignificant to affect the fatigue crack growth.

NEW CONCEPTS FOR FATIGUE THRESHOLDS

Since closure is not a major factor for crack advance, we have analyzed the fatigue data of many different materials taken from the literature and arrived at the following conclusions:- (1) to completely define fatigue, we need two independent load parameters ΔK & K_{max} , and not one, ΔK , that is commonly used; (2) this leads to two thresholds, one critical cyclic stress intensity amplitude ΔK_{th}^* and a critical maximum stress intensity K_{max}^* ; (3) these two parameters are needed to be satisfied simultaneously for crack growth to occur; (4) the entire fatigue data of ΔK_{th} vs R dependence can be fully explained without invoking closure, in terms of these two parameters. In the limited R regions, one or the other parameter controls crack growth while both critical values are being met (see Fig.1a, for alloy Ti-6Al-4V,ref.(8)); (5) at low R, fatigue is K_{max} controlled meaning that ΔK_{th} increases with decreasing R to meet the required K_{max}^* . Similarly, at high R values, fatigue is ΔK_{th} controlled and K_{max} has to increase to meet the required ΔK_{th}^* ; (6) both these critical parameters can be determined by plotting ΔK_{th} versus K_{max} (as in Fig.1b). This plot provides the interrelation between the two driving force parameters mapping the regimes where the cyclic loads are damaging (shaded region) and where they are not (below the curve); (7) physically, ΔK_{th}^* provides the minimum cyclic amplitude required to establish a characteristic fatigue damage and K_{max}^* provides the critical stress required to break open the crack-tip bonds in the fatigue damaged region. Fig.1b provides a plot showing the interdependence of these two parameters to ensure the conditions necessary for fatigue crack growth; (8) these two critical parameters are dependent on the microstructure, slip mode and crack tip environment; for example, with an increasing aggressiveness of the crack tip environment (oxygen, hydrogen, water vapor or NaCl) the role of K_{max}^* becomes increasingly important than ΔK_{th}^* , since the environment affects the crack tip bonds more than the

- (3) Vasudevan, A. K., Sadananda, K. & Louat, N., *Scripta Metall. et Materialia*, vol.28, 1993, p. 837.
- (4) Vasudevan, A. K., Sadananda, K. & Louat, N., (invited review) *Mater. Sci. Eng*, 1994, in press.
- (5) Sadananda, K. & Vasudevan, A. K., *ASTM STP - 1220*, 1994, in press.
- (6) Louat, N., Sadananda, K., Duesbery, M. S. & Vasudevan, A. K., *Metall. Trans.*, vol. 24A, 1993, p.2225.
- (7) Suresh. S, "Fatigue of Materials", Cambridge University Press, 1991.
- (8) Doker, H and Marci, G, *Int. J. of Fatigue*, vol. 5, 1983, p. 187.
- (9) Beevers, C. J., " Some Aspects of the Influence of Microstructure and Environment on ΔK Thresholds", *Fatigue Thresholds Proceedings*, Stockholm, Edited by J. Backlund, A. F. Blum and C. J. Beevers, EMAS, Wasrley, UK, 1981, p. 257.
- (10) Stewart, A. T., *Engg. Fract. Mech.*, vol.13, 1980, p.463.
- (11) Blom, A. F., " Near-Threshold Fatigue Crack Growth and Crack Closure in 17-4 PH Steel and 2024-T3 Aluminum Alloy", *Proceedings "Fatigue Crack Growth Threshold Concepts "*, Edited by D. Davidson and S. Suresh, AIME, 1984, p.263.
- (12) Vasudevan, A. K. and Sadananda, S., *Metallurgical and Materials Transactions*, 1994, in press.

corresponding ΔK vs K_{\max} plot is shown in Fig.5b. The alloy selected for the example above shows that the hydrogen assisted type of fatigue behavior at low growth rates near thresholds (10^{-8} m/cycle) changes over to the crack-tip blunting type of behavior at high growth rates ($>10^{-6}$ m/cycle) where the identification of the critical stress K^*_{\max} becomes difficult. As the crack growth rates increase rapidly, K_{\max} component becomes increasingly dominant. Thus as the behavior changes from Class-IV to Class-I, the role of plasticity increases with concomitant decrease of the role of environment. This is illustrated in Fig.3b schematically, where the relative mechanisms are listed.

SUMMARY

We have shown that fatigue crack growth is a two-parametric problem. There are two thresholds that must be satisfied simultaneously for a crack to advance, a concept that is independent of the existence of crack closure. The two driving forces should be related to microstructure, slip modes and environment. The entire fatigue crack growth behavior was classified into main five classes, each class being controlled by a given fatigue crack growth process. The concepts also suggest that for a complete fatigue description it is necessary to get a systematic set of data at various load ratios and crack growth rates. Detailed description of the fatigue behavior is given in references (1-6) and that on the classification scheme is discussed in (12).

REFERENCES

- (1) Vasudevan, A. K., Sadananda, K. & Louat, N., Scripta Metall. et Materialia, vol.27, 1992, p. 1673.
- (2) Vasudevan, A. K., Sadananda, K. & Louat, N., Scripta Metall. et Materialia, vol.28, 1993, p.65.

it converges to Class-III when the intercept goes to zero. Class-IV (shown with two differing slopes) corresponds to the type when ΔK_{th} intercept at $R=1$ is less than zero. Experimentally the curve may level off before ΔK_{th} can approach zero, as in Fig.3a. For the sake of understanding, we extrapolate the ΔK_{th} vs R curves to $R=1$ to give us the basis for the classification. Thus, as the degree of environmental effect increases, the slope of the ΔK_{th} vs R curve becomes steeper, moving from Class-I behavior (such as in inert environment) towards the Class-IV that corresponds to an aggressive environment (Fig.3a). Class-II behavior is observed in pure materials (low strength, high ductility) and in some of the medium/high strength steels where crack-blunting process is prevalent. Class-III behavior is common in most aluminum-base alloys under aqueous environment. Here, ΔK_{th} and K_{max} are uniquely defined. Class-IV behavior is not very common, but is observed in a few high strength materials that exhibit purely environmental controlled fatigue, such as in steels that are susceptible to hydrogen-assisted crack growth. Thus the physics of crack growth process in different classes of behavior is affected by the degree of aggressiveness of the crack-tip environment. The experimental evidence for such a classification is shown in the Fig.4a, in terms of ΔK_{th} vs R plot and the corresponding ΔK_{th} vs K_{max} plot in Fig.4b. The data is obtained from various materials, the references are given elsewhere (4-6). One can see the similarity between the experimental data in Fig.4 to the trends in the hypothetical curves in Fig.3.

So far we have discussed the fatigue crack growth trends at the near threshold regime. We can extend the classification scheme to higher crack growth rates. To show this, we have chosen an example from Class-IV material behavior. As the modification of the material behavior changes with growth rates, the classification hierarchy moves towards the lower classes. This is illustrated by considering the data from SA342-2 alloy steel that is sensitive to the hydrogen assisted fatigue crack growth at the near threshold region (7). Fig.5a indicates this point, where ΔK dependence on R at various growth rates is shown starting from the near threshold region 10^{-8} m/cycle to 10^{-5} m/cycle, along with the $\Delta K - R$ extrapolation to $R=1$ to show the relative classifications. The

fatigue damage zone ahead of the crack tip. This is shown in the Fig.2, in terms of ΔK_{th}^* vs K_{max}^* plot for various materials(2). Here, in going from the vacuum to moisture, the slope of the plot decreases dramatically with increasing environmental aggressiveness, finally approaching the stress corrosion fatigue crack growth (shown by the dotted line). It is interesting to note that all the available vacuum data lie on a single line irrespective of the material composition, slip mode, strength, modulus etc. Similarly, all the lab air results are clustered around another line with a lower slope than the one for vacuum. There is more scatter in the ambient air data and could be due to variations in the relative humidity.

CLASSIFICATION OF FATIGUE CRACK GROWTH

Based on the variation of ΔK_{th} vs R relation, in terms of the slope and intercepts for $R > 0$, it is possible to conceive five different classes (Class I-V) of material behavior under fatigue loading, as shown schematically in Fig.3. We shall restrict our discussions to threshold regime of Classes I through IV only, as it relates mostly to metallic systems. Polymeric systems fall under Class-V which is omitted from Fig.3. The basic concepts are applicable to fatigue behavior from near threshold region for all crack growth rates. Such a classification helps us to recognize the individual fatigue behavior of different families of materials and to understand the relative role of environment on fatigue. For convenience only, we have taken all the curves to start from the same ΔK_{th} value at $R=0$, in Fig.3.

The basic classification is schematically illustrated in Fig. 3a. Here we label a material to be behaving as "normal", if the extrapolation of the linear portion of the ΔK_{th} vs R curve (Fig.3a) intersects the R-axis at $R=1$ with $\Delta K_{th}=0$. This class of materials is designated as Class-III. When ΔK_{th} becomes independent of R for all $R > 0$, that material is classified as Class-I behavior, with the slope approaching zero. If the ΔK_{th} intercept at $R=1$ is greater than zero, we have termed it as Class-II. In the Fig.3a, two different slopes are shown for Class-II (such as IIa & IIb). In the limit, Class-II converges to Class-I when the ΔK_{th} - R slope becomes zero and

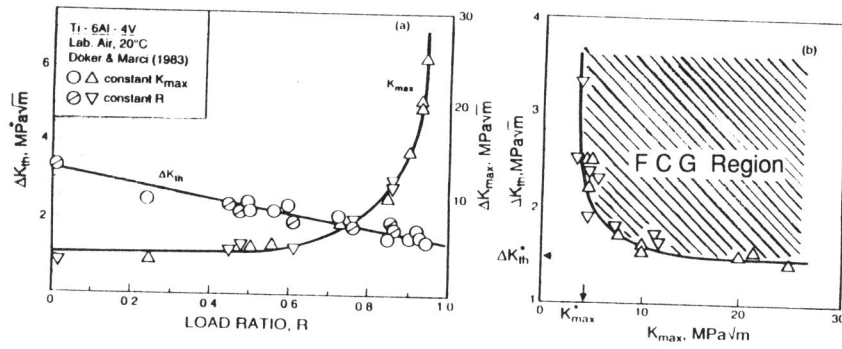


Figure 1 : (a) Variation of ΔK_{th} and K_{max} with load ratio R for Ti-6V-4Al alloy in lab air, and (b) a replot of (a) as K_{max} dependence on ΔK_{th} .

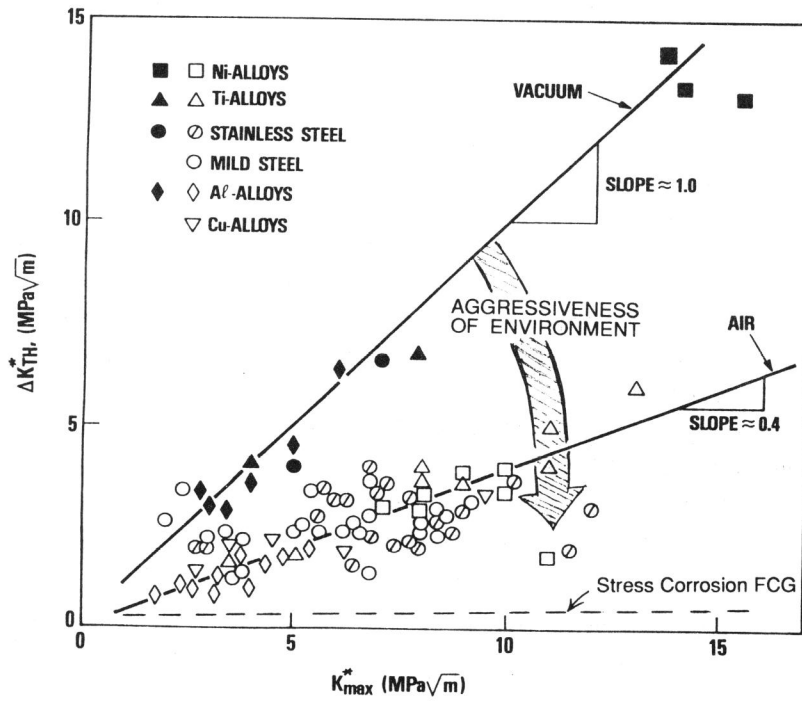


Figure 2 : Variation in ΔK_{th}^* and K_{max}^* for various materials in vacuum and lab. air environment.

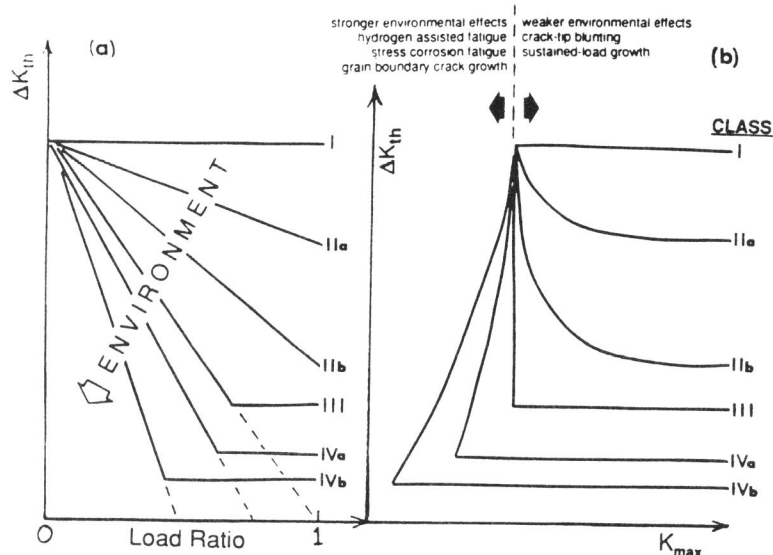


Figure 3 : Schematic illustration of the overall fatigue mechanisms to show the four major classifications in terms of (a) ΔK_{th} vs R , and (b) ΔK_{th} vs K_{max} , along with the regions affected by the environment.

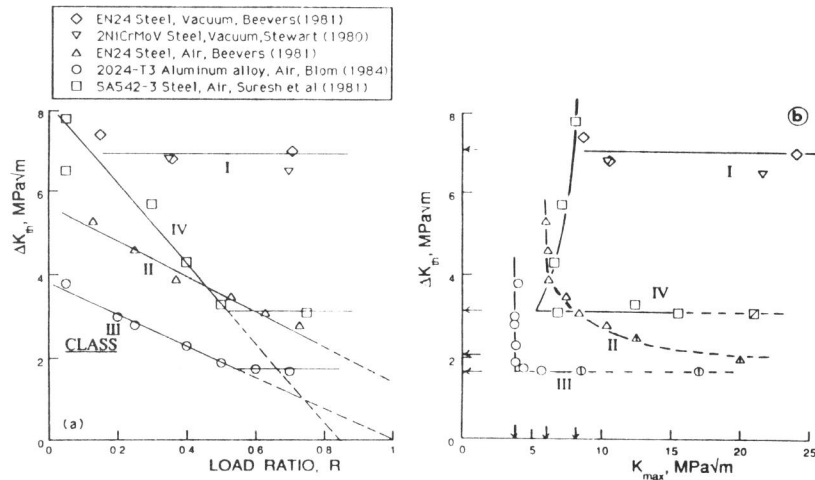


Figure 4: Experimental results depicting the different class of fatigue behavior in terms of (a) ΔK_{th} vs R , and (b) ΔK_{th} vs K_{max} . The data was taken from aluminum and steel alloys.

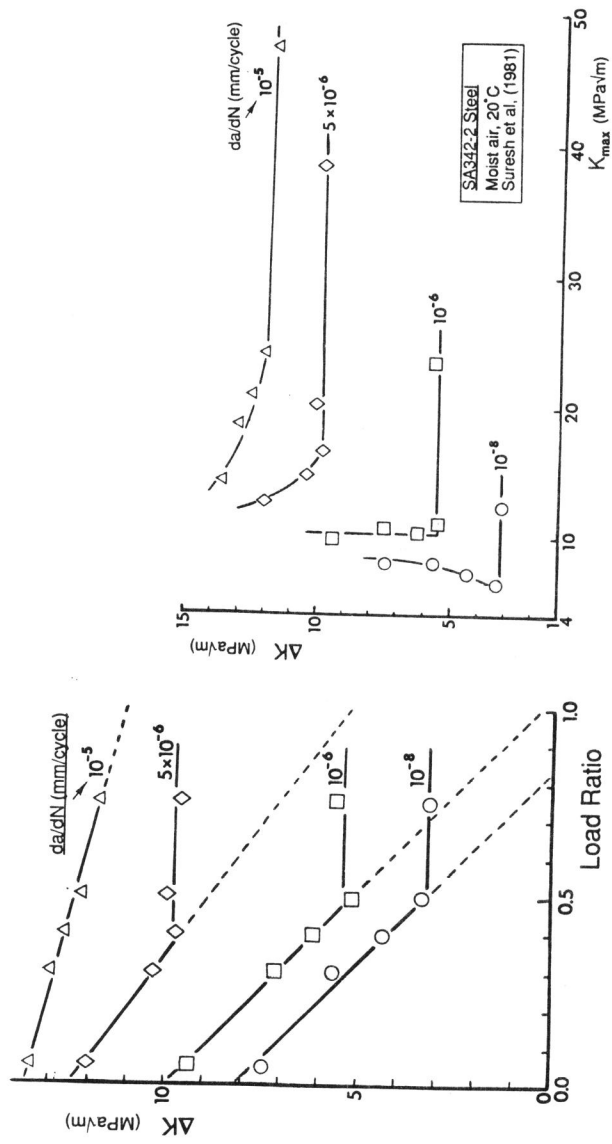


Figure 5: Class IV steel data extended to higher crack growth rates showing the transitions from Class-IV to III to II; (a) ΔK_{th} vs R, and (b) ΔK_{th} vs K_{max} .